Table DR1. Selected electron probe microanalyses (in wt.%) of minerals in samples RO172B and RC168

Sample	Garnet-Spinel mylonite RC168								Garnet peridotite RO172B								
									Neoblasts					Porphyroclast Core			
Mineral	Ol (grt)	Ol (neo)	Opx (bast)	Cpx (neo)	Sp (grt)	Sp (neo)	Grt (por)	Grt (neo)	Ol	Opx	Cpx	Sp	Grt (Ke)	Ol	Opx	Cpx*	Grt
SiO_2	40.0	40.0	*na*	52.9	bd	bd	41.4	41.5	39.9	55.7	52-3	0.21	*na*	40.3	55.2	52.3	42.1
TiO_2	*na*	*na*	*na*	0.2	*na*	*na*	bd	bd	*na*	0.08	0.78	0.05	*na*	*na*	0.13	1.50	bd
Al_2O_3	*na*	*na*	*na*	6.2	52.5	52.7	22.8	23.1	*na*	2.20	6.9	51.2	*na*	*na*	3.20	8.1	23.2
Cr_2O_3	*na*	*na*	*na*	1.00	15.2	15.3	0.85	0.99	*na*	bd	0.37	15.4	*na*	*na*	0.58	0.62	0.39
FeO	11.6	11.8	*na*	2.47	14.2	12.9	10.62	9.48	12.7	8.07	3.14	14.3	*na*	13.2	7.97	3.00	9.49
MnO	0.2	0.1	*na*	0.53	0.19	0.13	0.75	0.75	0.17	0.17	0.09	0.23	*na*	0.17	0.13	0.01	0.29
MgO	48.2	47.3	*na*	14.9	17.4	18.2	19.2	20.3	46.8	33.4	13.7	17.2	*na*	46.4	32.8	13.3	19.8
CaO	bd	bd	*na*	19.7	*na*	*na*	4.51	4.73	bd	0.34	19.1	na	*na*	bd	0.44	18.4	4.86
Na_2O	*na*	*na*	*na*	1.98	*na*	*na*	*na*	*na*	*na*	0.02	2.53	na	*na*	*na*	0.07	2.84	na
Total	100.0	99.1	*na*	99.9	99.6	99.3	100.1	100.5	99.7	100.0	99.0	98.5	*na*	100.0	100.5	99.7	100.2

Cpx= clinopyroxene; Grt= garnet; Ol= olivine; Opx= orthopyroxene; Sp= spinel; *na* = non-analysed; bd = below detection limit; bast= altered to bastite; Ke= garnet transformed to kelyphite; neo = neoblast; por= porphyroclast. In sample RC168 the grt enclosed in parentheses(grt) indicates that analyses were made in grains with adjacent fresh garnet. (*). Clinopyroxene occuring as small tabular inclusions within a garnet porphyroclast (Fig. 2A; inclusion labeled Cpx). Mineral analyses were performed on a CAMECA SX1000 electron microprobe at the University of Granada. Operating conditions were: acceleration voltage of 15eV, beam current of 15 nA and beam diameter of 5 µm. Natural and synthetic mineral and glasses were used as standards.

SAMPLE RC168: The forsterite content of olivine is rather homogeneous (Fo= 87-88) both in olivine adjacent to larger garnet porphyroclasts [Ol(grt); Table DR1; Fig. 2 D & E] and in olivine neoblasts in the recrystallized mylonitic matrix [Ol(neo); Table DR1; Figs. DR1 B-D]. The X_{Cr} of spinel ranges from 0.16 to 0.19 and display the same compositional range in large anhedral spinel surrounding garnet porphyroclast (Fig. 2D) or surrounded by garnet (Fig. 2E) [Sp(grt); Table DR1], and in elongated spinel neoblasts associated with garnet neoblasts in the recrystallized mylonitic matrix (Fig. DR1 B-D) [Sp(neo); Table DR1]. Garnet is rich in pyrope component [Pyr =69-72; Alm= 0.13-0.17; Grs= 0.12-0.13)] and shows a similar composition in large garnet porphyroclasts (Fig. DR1 A) [Grt(por) in Table DR1] and in garnet neoblasts surrounded by kelyphite (Figs. DR1 C & D) in the recrystallized mylonitic matrix [Grt(neo) in Table DR1]. Orthopyroxene occurs as elongated neoblasts altered to bastite (pseudomorphic serpentine) (Fig. DR2). Clinopyroxene is Cr_2O_3 rich (c. 1.0 wt% Cr_2O_3) and shows a rather constant and high X_{Mg} (0.90-0.91).

SAMPLE RO172B: Olivine, occurring either as inclusions, adjacent to garnet (Fig. 2 B & C) or as neoblasts in the recrystallized matrix (Fig. 2 A), displays a rather constant forsterite content (Fo= 86-87). The MgO, FeO, Cr_2O_3 and CaO content of garnet porphyroclast (Fig. 2D) is constant over a large distance at garnet cores, and decreases (MgO, Cr_2O_3 and CaO) or increases (FeO and X_{Mg}) towards the grain rims (compositional profiles are shown in Fig.

DR2). The pyrope content at the core of garnet porphyroclasts ranges from 68 to 67, and decreases (Py= 65-66) towards the garnet rims adjacent to orthopyroxene. The MgO, FeO and Al_2O_3 content at the core of orthopyroxene porphyroclasts adjacent to garnet is rather constant over a large distance (Fig. DR2). The Al_2O_3 content at orthopyroxene porphyroclast core is low (4-3 wt.%), and decreases towards the grain rims (Fig. DR2). Orthopyroxene porphyroclast cores display a restricted variation of X_{Mg} (0.86-0.88), which increases towards the orthopyroxene rims. The CaO content across orthopyroxene porphyroclasts is highly variable (0.39-0.64 wt.%) due to pervasive exsolution of secondary clinopyroxene (Fig. DR2). Clinopyroxene inclusions (c. 100 μm thick) in garnet have a greater TiO_2, Al_2O_3, and Na_2O content than clinopyroxene neoblasts in the recrystallized matrix (Table DR1). The X_{Cr} of elongated spinel neoblasts associated to kelyphite in the recrystallized mylonitic matrix (Fig. 2 A) ranges from 0.17-0.19, a similar X_{Cr} range to spinel neoblasts in Grt-Sp mylonite RC168.

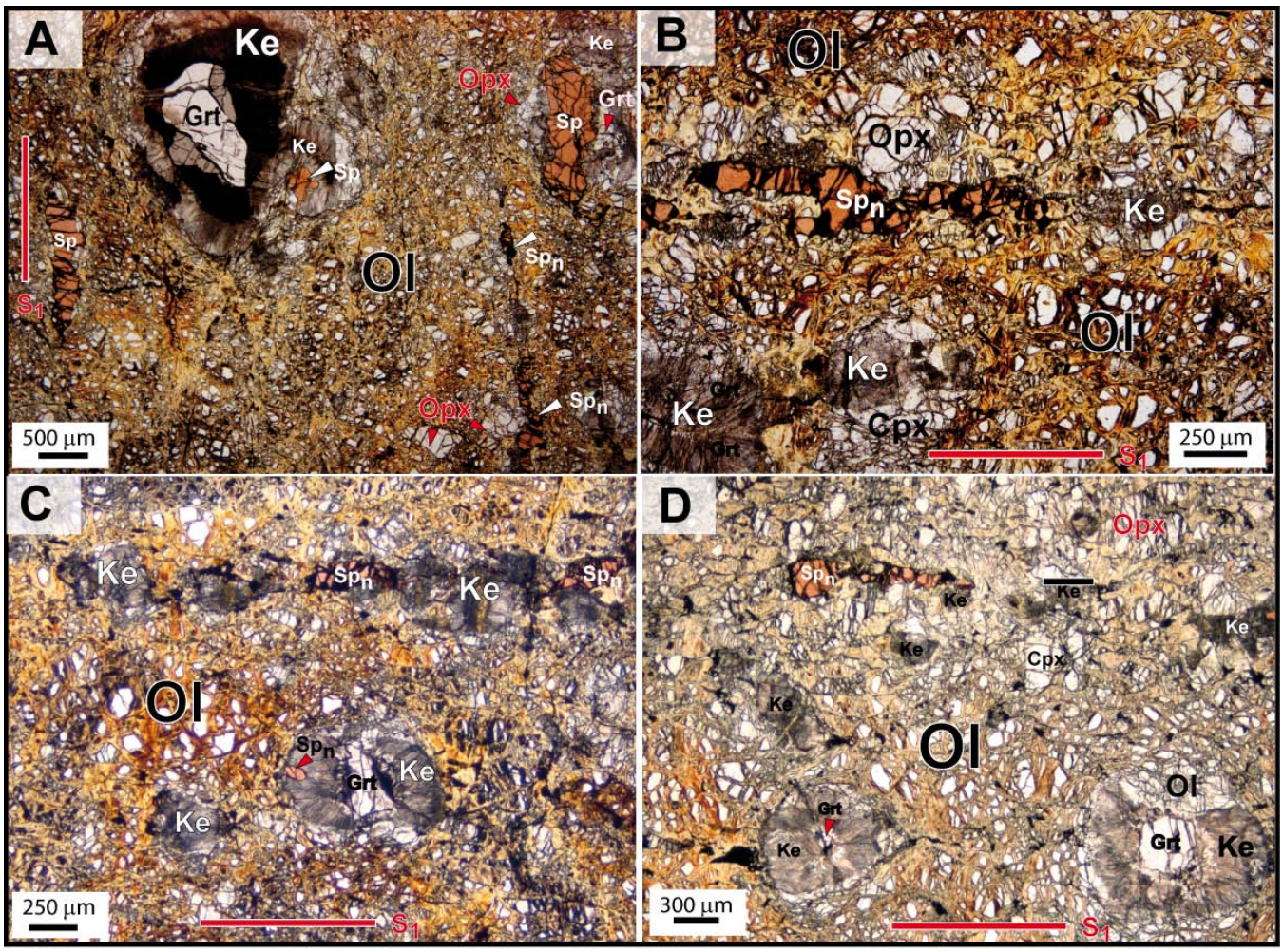

Figure DR1. Plane polarized micrographs illustrating the textural relationships between garnet-and spinel in Grt-Sp mylonite RC168. (A) Large garnet and adjacent spinel embedded in a fine recrystallized matrix of olivine, orthopyroxene, spinel, garnet-derived kelyphite and garnet neoblasts. (B) Close up of the recrystallized mylonitic matrix (Fig. DR1 A, right bottom corner) showing the textural relationships between, olivine and pyroxene neoblasts, and elongated spinel neoblasts (Sp_n) intermixed with garnet-derived radial aggregates of kelyphite. (C & D) Further details of the textural relationships in the recrystallized mylonitic matrix formed by olivine and pyroxene, garnet -partially or totally transformed to radial kelyphite- and elongated spinel neoblasts. The red line labeled S_1 is the trace of the mylonitic foliation. Ol= olivine; Ke= kelyphitic aggregates; Sp= spinel; Sp_n= elongated spinel neoblasts; Opx= orthopyroxene; Cpx= clinopyroxene.

Textural description: Olivine in Grt-Sp mylonite RC168 occurs mostly in the mylonitic matrix as recrystallized olivine neoblasts with grain size ranging from 100 to 500 µm. Orthopyroxene -altered to bastite- occurs as neoblasts (400-100 µm) aligned parallel to the mylonitic foliation and spatially associated with garnet (partially or totally transformed to radial kelyphitic aggregates), with large spinel adjacent to garnet porphyroclasts (Fig. DR1 A) and with elongated spinel neoblasts (Fig. DR1 B). Large garnet porphyroclasts (ranging from 1 to-3 mm in size) are aligned parallel to the mylonitic

foliation (Figs. 2E-F & Fig. DR1 A) and are partially transformed to concentrically zoned kelyphite (a fine-grained symplectitic mixture of orthopyroxene, spinel, olivine, plagioclase, and ilmenite; see Obata, 1994 for a detailed description of garnet derived kelyphite in Ronda peridotite). Most garnet porphyroclasts occur as single round grains, or associated to spinel with sharp contacts between both phases (Figs. 2E-F; Fig. DR1 A); spinel– fresh garnet intergrowth occurs as anhedral or weakly elongated spinel that either is surrounded by garnet (Fig. 2E) or, more commonly, is surrounding garnet adjacent to olivine and orthopyroxene (Figs. 2F & DR1 A). Non-elongated spinel surrounding garnet partially transformed to kelyphite is also common around garnet porphyroclasts (Fig. DR1 A) and neoblasts (Fig. DR2C). Garnet neoblasts (50-600 μm in size) occur in the recrystallized mylonitic matrix as round grains partially (Fig. DR1 C & D) or totally (Fig. DR1 B) transformed to radial kelyphitic aggregates. Only the core of larger garnet neoblasts (> 300 um) preserve fresh relics of garnet (Figs. DR1 C & D). Garnet neoblasts (or garnet-derived kelyphite) are in textural contact with the recrystallized olivine (Fig. DR1 D), pyroxene and elongated spinel neoblasts (Figs. DR1 B-C). Spinel grains in the recrystallized matrix (50-125 μm thick) are elongated, with their long axis parallel to the mylonitic foliation, and intermixed with orthopyroxene (Figs. DR1 B & D), olivine, radial aggregates of kelyphite (50-200 μm thick) (Fig. DR1 B-D) of garnet neoblasts (Fig. DR1 C).

Significance of Grt-Sp textural relationships: We interpret sGrt-Sp textures in mylonitic sample RC168 as a snapshot of the synkinematic breakdown of Grt+Ol to a Opx+Cpx+Sp+Grt assemblage. The garnet porphyroclast -surrounded by pyroxene and olivine (Fig. 2E & DR1 A)- are aligned along the foliation plane demonstrating the prekinematic nature of the garnet porphyroclastic assemblage. Larger spinel and orthopyroxene adjacent to garnet porphyroclast are interpreted as the reaction products of garnet around more competent, large garnet porphyroclasts. With the progress of garnet breakdown and consumption, garnet and spinel are sinkynematically incorporated into a fine matrix composed of elongated spinel and garnet neoblasts aligned parallel to the Grt-Sp mylonitic foliation (red line labeled S_1). The synkinematic nature of this transformation is attested by the progressive stretching of spinel neoblasts (Sp_n) associated to smaller garnet neoblasts, both in textural contact with olivine and pyroxene neoblasts in the recrystallized mylonitic matrix (Fig. DR1 B-D). The similarity in composition of spinel associated with garnet porphyroclasts and spinel neoblasts in the recrystallized matrix (Table DR1), the pyrope-rich conten of garnet (Table DR1; see also Obata, 1980; 1982) (Figs. 2E & DR1 C) and the constant and high Fo-content of olivine, indicate overall mineral equilibration at the Grt-Sp lherzolite transition for the bulk composition of sample RC168 (1.9-2.0 GPa).

Several observations demonstrate that kelyphite aggregates after garnet in Ronda Grt-Sp mylonites are post-kinematics and postdate the formation of the Grt-Sp mylonite assemblages. Obata (1994) showed that kelyphite after garnet in Ronda was formed at 620-700 ^{o}C and 0.4-0.8 GPa during crustal emplacement of peridotites. Such pressure range is well below the pressure required for the preservation of pyrope-rich garnet neoblasts in textural contact with olivine neoblasts (c. 2 GPa in sample RC168). On the other hand, the crystal preferred orientation of olivine in Grt-Sp mylonites requires ductile deformation and the operation of combined grain boundary sliding and dislocation creep deformation mechanisms in olivine only operative at temperatures above 850 ^{o}C (Precigout et al, 2007; Soustelle et al., 2009). The postkinematic nature of kelyphite is further supported by the radial and undeformed shape of the fine kelyphite aggregates surrounding garnet porphyroclasts and

neoblasts or occurring as isolated kelyphitic aggregates in the mylonitic matrix (Figs. DR1 B-D) (see also Van der Wal and Vissers, 1996; 1997).

REFERENCES

Obata, M., 1980, The Ronda peridotite -garnet-lherzolite, spinel-lherzolite, and plagioclase-lherzolite facies and the P-T trajectories of a high-temperature mantle Intrusion: Journal of Petrology, v. 21, p. 533-572.

Obata, M., 1982, Reply to W. Schubert's comments on "The Ronda peridotite - garnet-lherzolite, spinel-lherzolite, and plagioclase-lherzolite facies and the P-T trajectories of a high-temperature mantle intrusion": Journal of Petrology, v. 23, p. 296-298.

Obata, M., 1994, Material transfer and local equilibria in a zoned kelyphite from a garnet pyroxenite, Ronda, Spain: Journal of Petrology, v. 35, p. 271-287.

Precigout, J., Gueydan, F., Gapais, D., Garrido, C.J., and Essaifi, A., 2007, Strain localisation in the subcontinental mantle -a ductile alternative to the brittle mantle: Tectonophysics, v. 445, p. 318-336.

Soustelle, V., Tommasi, A., Bodinier, J.L., Garrido, C.J., and Vauchez, A., 2009, Deformation and reactive melt transport in the mantle lithosphere above a large-scale partial melting domain: the Ronda peridotite massif, Southern Spain: Journal of Petrology, v. 50, p. 1235-1266.

Van der Wal, D., and Vissers, R.L.M., 1996, Structural petrology of the Ronda peridotite, SW Spain: Deformation history: Journal of Petrology, v. 37, p. 23-43.

Van der Wal, D., and Vissers, R.L.M., 1997, Reply to Discussion by H. P: Zeck of 'Structural petrology of the Ronda Peridotite, SW Spain; deformation history': Journal of Petrology, v. 36, p. 534-536.

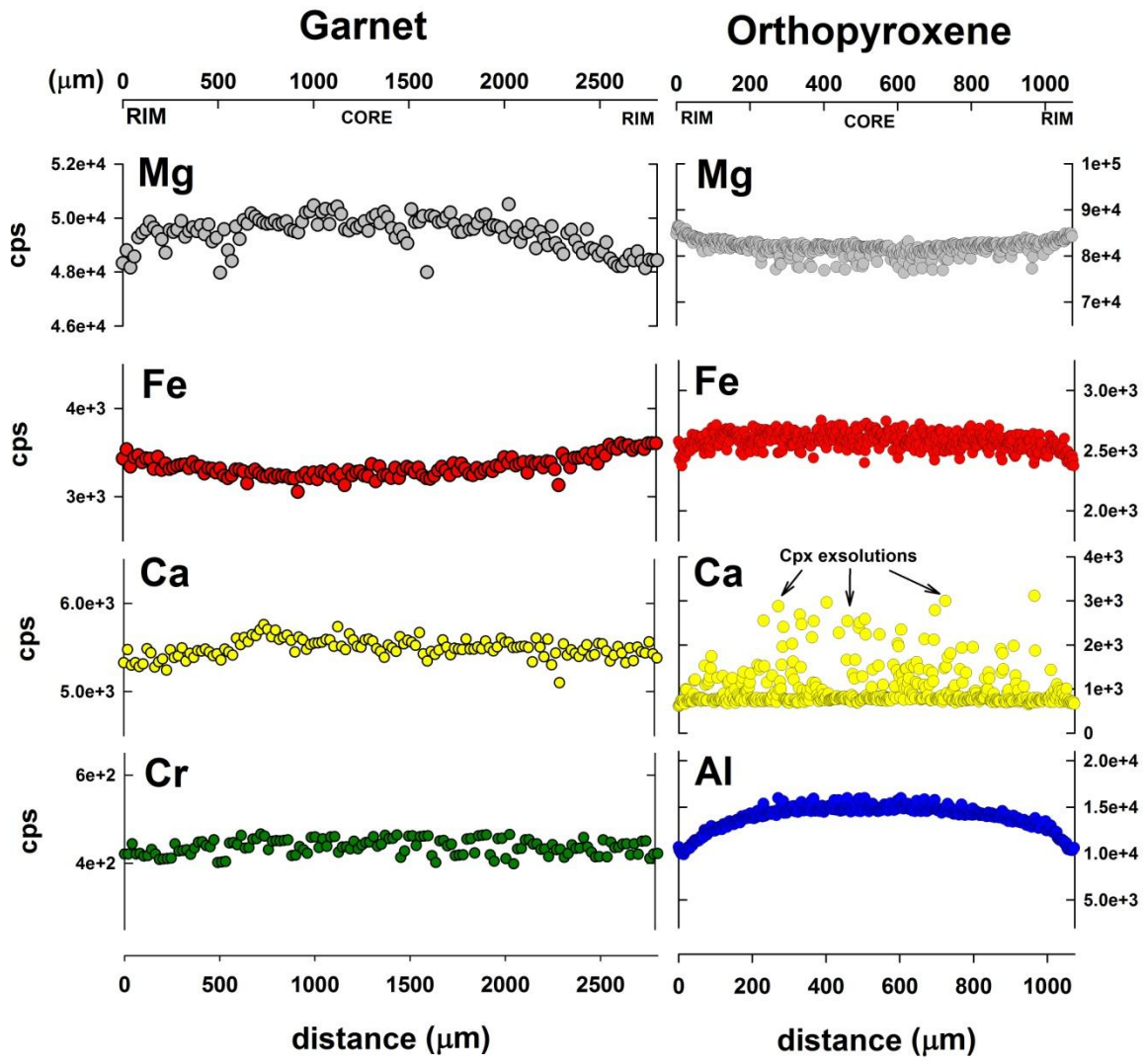

Figure DR2. Compositional profiles across garnet (left) and adjacent orthopyroxene (right) porphyroclasts in garnet lherzolite assemblages from sample RO172B (cf. Fig. 2A). Garnet profile shows high Mg/Fe ratios in the grain core, and decreasing Mg/Fe towards the grain rims. Orthopyroxene shows a complementary Mg-Fe zoning to garnet, with Mg and Fe plateaus in the cores, and an increase of Mg and a decrease of Fe towards the rims. Ca and Cr slightly decrease towards the garnet rims. Al in orthopyroxene shows a nearly flat profile in the cores and a rimward decrease. Fe, Mg and Al zoning patterns are consistent with partial reequilibration under cooling in the garnet lherzolite facies. The slight increase in Al in the outermost Opx rims may have developed during final decompression. Ca spikes in orthopyroxene -common in garnet peridotites (e.g. Becker, 1997)- are due to pervasive tiny clinopyroxene exsolution lamellae (several microns thick) formed during retrograde cooling (e.g. Obata, 1980; Becker, 1997; Medaris and Carswell, 1990 and references therein).

Analytical Conditions: Elemental variations (cps =counts per second) were obtained by Energy Dispersive X-ray Spectroscopy (EDS) in a CAMECA SX 100 electron superprobe at the CIC of the University of Granada (Granada, Spain). Accelerating voltage and beam current intensity were 15.1 KeV and 99 nA, respectively. Spectra were taken on the Kα line of the spectrum of each element, with a

dwell time of one second on each step. The step size is 20 μm for garnet profile (138 points), and 3 μm for the orthopyroxene profile (444 points).

REFERENCES

Becker, H., 1997, Petrological constraints on the cooling history of high-temperature garnet peridotite massifs in lower Austria: Contributions to Mineralogy and Petrology, v. 128, p. 272-286.

Medaris, L.G., Carswell, D.A., 1990. The petrogenesis of Mg–Cr garnet peridotites in European metamorphic belts. In: Carswell, D.A. (Ed.), Eclogite Facies Rocks. Blackie, Glasgow, p. 260–290.

Obata, M., 1980, The Ronda peridotite -garnet-lherzolite, spinel-lherzolite, and plagioclase-lherzolite facies and the P-T trajectories of a high-temperature mantle Intrusion: Journal of Petrology, v. 21, p. 533-572.